Article

Neuron

Neural Basis of Cognitive Control over Movement Inhibition: Human fMRI and Primate Electrophysiology Evidence

Highlights

- A context-dependent stop-signal task with human fMRI and primate neurophysiology
- Task design, data types, and analysis methods enable dissociation of system components
- Multiple distinct parts of rVLPFC and interactions with other brain areas required
- Context-based attention, interpretation, monitoring, but not direct response control

Authors

Kitty Z. Xu, Brian A. Anderson, Erik E. Emeric, Anthony W. Sali, Veit Stuphorn, Steven Yantis, Susan M. Courtney

Correspondence

kitty.zhexu@gmail.com (K.Z.X.), brian.anderson@tamu.edu (B.A.A.), erik.emeric@gmail.com (E.E.E.), anthony.sali@duke.edu (A.W.S.), veit@jhu.edu (V.S.), courtney@jhu.edu (S.M.C.)

In Brief

Xu et al. present a rare combination of complementary evidence from human fMRI and primate neurophysiology, demonstrating that response inhibition is not directly accomplished by the rVLPFC, but instead requires multiple, distinct rVLPFC networks involving attention and contextual stimulus interpretation.

Xu et al., 2017, Neuron *96*, 1447–1458
December 20, 2017
https://doi.org/10.1016/j.neuron.2017.11.010

CellPress

Neuron
Article

Neural Basis of Cognitive Control over Movement Inhibition: Human fMRI and Primate Electrophysiology Evidence

Kitty Z. Xu,[1,2,*] Brian A. Anderson,[1,3,*] Erik E. Emeric,[4,*] Anthony W. Sali,[1,5,*] Veit Stuphorn,[4,*] Steven Yantis,[1,7] and Susan M. Courtney[1,4,6,8,*]
[1]Department of Psychological & Brain Sciences, Johns Hopkins University, Baltimore, MD 21218, USA
[2]Pinterest, Inc., San Francisco, CA 94701, USA
[3]Department of Psychology, Texas A&M University, College Station, TX 77843, USA
[4]Department of Neuroscience, Johns Hopkins School of Medicine, Baltimore, MD 21205, USA
[5]Center for Cognitive Neuroscience, Duke University, Durham, NC 27708, USA
[6]F.M. Kirby Research Center for Functional Brain Imaging, Kennedy Krieger Institute, Baltimore, MD 21205, USA
[7]This author is deceased
[8]Lead Contact
*Correspondence: kitty.zhexu@gmail.com (K.Z.X.), brian.anderson@tamu.edu (B.A.A.), erik.emeric@gmail.com (E.E.E.), anthony.sali@duke.edu (A.W.S.), veit@jhu.edu (V.S.), courtney@jhu.edu (S.M.C.)
https://doi.org/10.1016/j.neuron.2017.11.010

SUMMARY

Executive control involves the ability to flexibly inhibit or change an action when it is contextually inappropriate. Using the complimentary techniques of human fMRI and monkey electrophysiology in a context-dependent stop signal task, we found a functional double dissociation between the right ventrolateral prefrontal cortex (rVLPFC) and the bi-lateral frontal eye field (FEF). Different regions of rVLPFC were associated with context-based signal meaning versus intention to inhibit a response, while FEF activity corresponded to success or failure of the response inhibition regardless of the stimulus response mapping or the context. These results were validated by electrophysiological recordings in rVLPFC and FEF from one monkey. Inhibition of a planned behavior is therefore likely not governed by a single brain system as had been previously proposed, but instead depends on two distinct neural processes involving different sub-regions of the rVLPFC and their interactions with other motor-related brain regions.

INTRODUCTION

A critical function of executive control is the ability to flexibly inhibit or change a plan of action when it is contextually inappropriate. Human lesion and functional neuroimaging studies have used a simple Stop Signal Task (SST) to demonstrate that the right ventrolateral prefrontal cortex (rVLPFC) is critical for stopping action. However, the specific function of rVLPFC activity in stopping is debated. While some argue for a direct role of rVLPFC in response inhibition (Aron et al., 2003), others have argued for a role of this region in either guiding attention to external events relevant to the task goal (Sharp et al., 2010; Corbetta and Shulman, 2002), or in encoding behaviorally relevant task rules (Koechlin et al., 2003). It is also possible that sub-regions of rVLPFC are responsible for each of the aforementioned functionalities, giving rise to its heterogeneous roles in cognitive control of movement inhibition (Levy and Wagner, 2011). For example, a more dorsal and posterior region, in or near the inferior frontal junction may have more stimulus processing and attention functions, while more ventral and anterior rVLPFC may be more directly involved in inhibiting or changing behavioral responses (Chikazoe et al., 2009; Verbruggen et al., 2010; Sebastian et al., 2016).

In a standard SST, participants execute a simple movement (e.g., saccade or button press) following an imperative go signal and have to cancel the planned movement when they receive an infrequent but highly salient stop signal. While the SST examines motor interactions between go and stop processes (Logan et al., 1984), it is also a cognitively demanding task that involves both attention and conflict resolution. The abrupt onset of a salient stimulus can result in a delayed response time even when that stimulus is irrelevant, an effect known as "attentional capture" (Yantis and Jonides, 1990; Yantis, 1993), and generally involves activation of brain regions implicated in attentional control (Serences et al., 2004, 2005). Furthermore, the anticipation of the possible appearance of the stop signal introduces a high degree of conflict and uncertainty—participants cannot know when the stop signal will be presented and whether they will be able to successfully stop (Botvinick et al., 2001, 2004). Taking these features into account, it can be difficult to separate out specific neural signals related to the cognitive demands involved in performing the SST from the neural signals related to motoric inhibitory control. A variant of the conventional SST utilizing so-called "continue" trials has been used to address these concerns (Sharp et al., 2010). The overall structure of the continue variant of the SST (or continue SST) is the same as the conventional SST, except that the continue signal instructs participants to

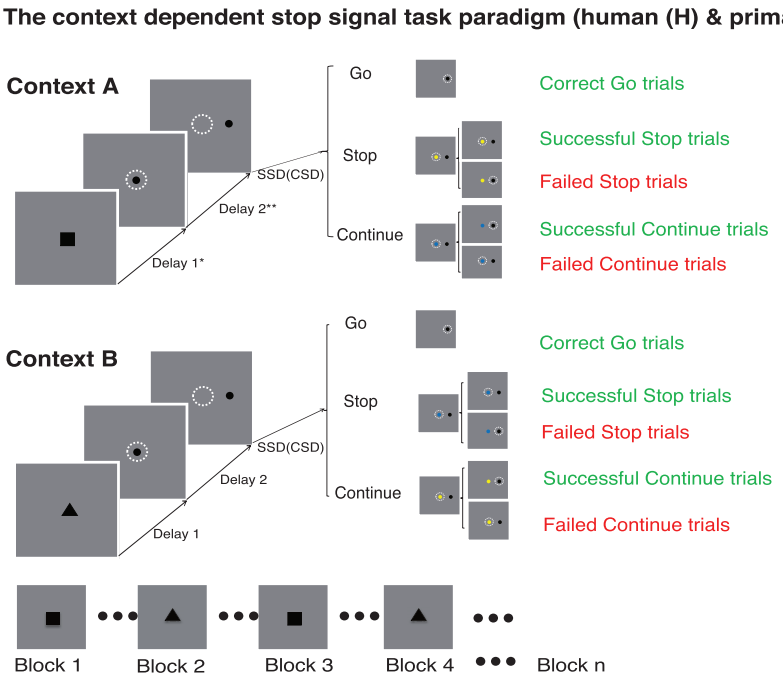

Figure 1. Context-Dependent Stop Signal Task

Human fMRI experiment: all trials started with a central context cue (triangle or square) on the screen for 500 ms. Next, the context cue disappeared and, simultaneously, a fixation cue appeared. After a variable delay, the fixation stimulus disappeared and a visual target appeared to the left or right, signaling participants to saccade to the target as quickly as possible. On Go trials (56% of all trials), the target appeared alone. In Stop trials (22%) and Continue trials (22%), a central stimulus (blue or yellow dot) was presented after a variable delay following the target onset (stop signal delay [SSD]; continue signal delay [CSD]; 4 fixed SSDs/CSDs ranged from 50 ms to 250 ms). The context alternated every 8, 10, or 16 trials, randomly and without prior warning. Primate electrophysiology experiment: all trials started with the monkey fixating at a central fixation spot for 200 ms (figure not shown), after which the fixation spot was replaced with a central context cue with either a square or a triangle shape. After the presentation of the central context cue for 350 ms, the cue was replaced by a central fixation spot. The remainder of the trial proceeded as in the human task with a visual target and the presentation of a stop or continue stimulus on 22% (44% total) of trials following a variable SSD/CSD. The context alternated at a fixed duration of either 50 or 100 trials per session.

proceed with the go response they were preparing. However, while the continue signal serves as an appropriate control for the attention-capture effect of the stop signal, it is not clear whether the continue signal also affects motor inhibitory control processes. In particular, processing the identity of the surprising signal (either continue or stop) takes time, and participants are likely to pause or delay the generation of their planned response in order to avoid making an error during this period of ambiguity, resulting in longer reactions times (RTs) on those trials. Here, we developed a task designed to more effectively decompose these components of motoric inhibition in order to better characterize the neural mechanisms underlying each.

We administered a context-dependent SST that incorporates oculomotor inhibition, attention capture and reorientation, and contextual rule encoding in one comprehensive experimental paradigm. Specifically, we aimed to test four alternative hypotheses regarding the functional organization of rVLPFC and its role in inhibitory control. Those hypotheses are: (1) rVLPFC is responsible for direct control of movement inhibition, (2) rVLPFC is responsible for reflexively reorienting attention to external stimuli that are behaviorally relevant, (3) rVLPFC is responsible for encoding task-relevant rules, and (4) sub-regions within rVLPFC contribute heterogeneous functions in movement inhibition. To fully address all four hypotheses, we used an approach that included human fMRI with univariate analysis, regions of interest (ROI)-based multi-variate pattern analysis (MVPA), and psychophysiological interactions (PPIs)-based functional connectivity analysis. Findings were further explored at the level of individual neurons by examining one monkey while the animal performed an equivalent SST as its human counterparts.

RESULTS

Behavioral Results

Healthy human participants (n = 21) performed a context-dependent SST, in which participants selectively generate, inhibit, or continue to generate a saccade, based on different signal colors and contexts that predefine the color-meaning association (Figure 1). Because the performance was comparable between contexts, behavioral data were collapsed across both contexts. The probability of making a saccade in Stop trials increased with increasing Stop signal delay (SSD), the time between the onsets of the target and the Stop signal, but remained relatively stable and high in Continue trials regardless of the Continue signal delay (CSD, Figure 2A). The mean reaction time (RT) in Failed Stop trials (262.24 ± 6.52 ms, mean ± standard error of mean [SEM]) was faster than in Go trials (289.25 ± 5.34 ms) but was the longest in Continue trials (321.28 ± 6.93 ms; Figure 2B). Pairwise comparisons showed that there was a significant difference between Go RT and Failed Stop RT ($t_{(20)} = 3.25$, $p = 0.0017$) and between Go RT and Continue RT ($t_{(20)} = -3.70$, $p < 0.001$).

Stop signal reaction time (SSRT) was estimated using the modified integration method (Mayse et al., 2014). This method provides an estimate of SSRT by directly comparing RT distributions in Stop trials and Go trials in order to determine the time point at which the Stop signal begins to slow down RTs relative to go trial RTs. Using the same method, we were also able to estimate the Continue signal reaction time (CSRT), which is the time it took participants to respond to the Continue signal and continue to make the saccade that they had planned. CSRT (111.58 ± 3.43 ms) and SSRT (118.72 ± 3.44 ms) were

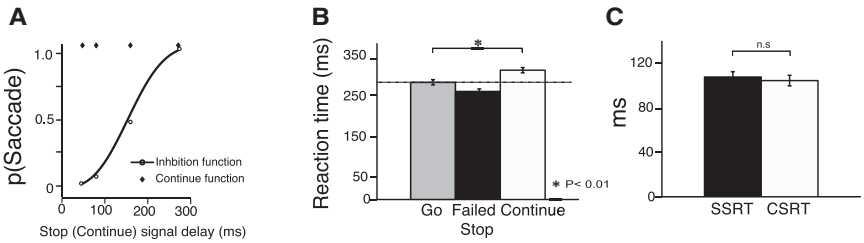

Figure 2. Behavioral Results for the Context-Dependent SST

(A) Inhibition function and Continue function for one exemplar behavioral session, with the probability that the participant generated a saccade as a function of the SSD/CSD. The black circles show raw inhibition function, and the black line shows Weibull-fitted inhibition function. The black diamonds show raw Continue function.

(B) Mean reaction time across all participants in Go (gray), Failed Stop (black), and Continue (white) trials.

(C) Mean Stop signal reaction time (SSRT, black) and Continue signal reaction time (CSRT, white). Error bars indicate SEM.

statistically indistinguishable ($t_{(20)} = -0.62$, $p = 0.55$; Figure 2C). These results suggest that the Continue signal and the Stop signal required a similar amount of time for visual processing and indistinguishably affected behavior.

fMRI Results

Using both voxelwise activation magnitude contrasts and MVPA, we attempted to identify whether any regions within the rVLPFC had activations that were consistent with any of the previously proposed functions of the rVLPFC.

Ventral rVLPFC Represents the Need to Stop

If rVLPFC is responsible for directly controlling movement inhibition, then greater BOLD activity in this area should be observed during successful stopping (SS) compared with when an eye movement was generated (e.g., either Go trials or Failed Stop [FS]). However, in contrast to these predictions, the ventral rVLPFC demonstrated elevated activity for both SS and FS trials when compared with Go trials (Figures 3B and 3C; Tables S1 and S2). Furthermore, MVPA was unable to reliably classify the pattern of BOLD activation between SS and FS trials in this region (accuracy = 53% ± 5%, $t_{(20)} = 0.71$, $p = 0.49$; darker gray bar for ventral rVLPFC in Figure 4). This suggests a role for this region of rVLPFC in representing the intention to stop, or in sending a response inhibition signal to FEF. The ventral rVLPFC could also be registering the presence of the Stop signal in order to monitor whether the response plan was cancelled appropriately. This region of rVLPFC, however, does not seem to be directly responsible for the actual inhibition of the movement.

Dorsal rVLPFC Represents a Behavioral Saliency Signal

One possible interpretation of the prior analysis of stop signal-related activity in the vLPFC, the magnitude of which was not related to whether inhibition was successful or unsuccessful (i.e., SS versus FS), would be that this activation reflects the processing of a salient signal (regardless of whether it was a stop or continue signal). If this interpretation were true, then the Continue signal should also elicit increased BOLD activation compared to Go trials, similar to that elicited by Stop trials. We further compared the BOLD activity in Continue trials versus Go trials in the same area of rVLPFC that demonstrated elevated activity for both SS and FS trials and observed no differential activation (Figures 3B and 3C; Table S1 and S2). This suggests that this particular region of rVLPFC specifically represented the presence of the Stop signal.

However, other sub-regions within rVLPFC might be involved in the detection of a salient, behaviorally relevant event regardless of its specific meaning. In this case, greater BOLD activity in this area should be observed during both Stop and Continue trials compared to Go trials, with the Stop and Continue signals eliciting a comparable magnitude of BOLD activation because they share identical sensory properties. Figure 3D (Tables S3 and S4) shows a part of rVLPFC that demonstrated elevated activity for Stop trials compared with Go trials, as well as elevated activity for Continue trials compared with Go trials. Furthermore, there was no activation magnitude difference between Stop and Continue trials (Figure 3E; Table S3 and S4), and MVPA was unable to classify SS versus FS in this region (accuracy = 53% ± 7%, $t_{(20)} = 0.47$, $p = 0.64$; darker gray bar for dorsal rVLPFC in Figure 4). Interestingly, the part of rVLPFC that showed elevated activity for both Stop and Continue trials was centered around the dorsal part of rVLPFC, distinct from the more ventral part of rVLPFC that showed elevated activity uniquely to Stop trials (Figure 3A). To further confirm that the activation patterns for Stop and Continue trials were different for these two regions of rVLPFC, we tested for a region by trial type interaction. A repeated-measures 2 × 2 ANOVA showed no main effect of region but did show a main effect of trial type and, importantly, a significant interaction effect ($p < 0.05$). We also tested whether the difference between the Stop and Continue activations was significantly different across the two regions using a paired t test, which was significant at $p < 0.01$.

Dorsal rVLPFC Represents Task Context

The mapping of color to response in the task was variable, such that each color signal served as the Continue signal or the Stop signal on different trials, depending on context. If rVLPFC is responsible for encoding context-based, task-relevant rules, then patterns of activation for Stop and Continue trials should be different, independent of the color of the signals. To test whether this region of activation in dorsal rVLFPC is responsible for simply detecting potentially relevant stimuli or actually codes the relevant rules for interpreting those stimuli, we performed an MVPA analysis. We were able to robustly classify the differential patterns of BOLD activation for the context-specific meaning of the signal (Stop versus Continue, accuracy = 70% ± 5%, $t_{(20)} = 4.09$, $p < 0.001$; light gray bar for dorsal rVLPFC in Figure 4A) but not the color of the signal (blue versus yellow, accuracy = 51% ± 4%, $t_{(20)} = 0.15$, $p = 0.88$).

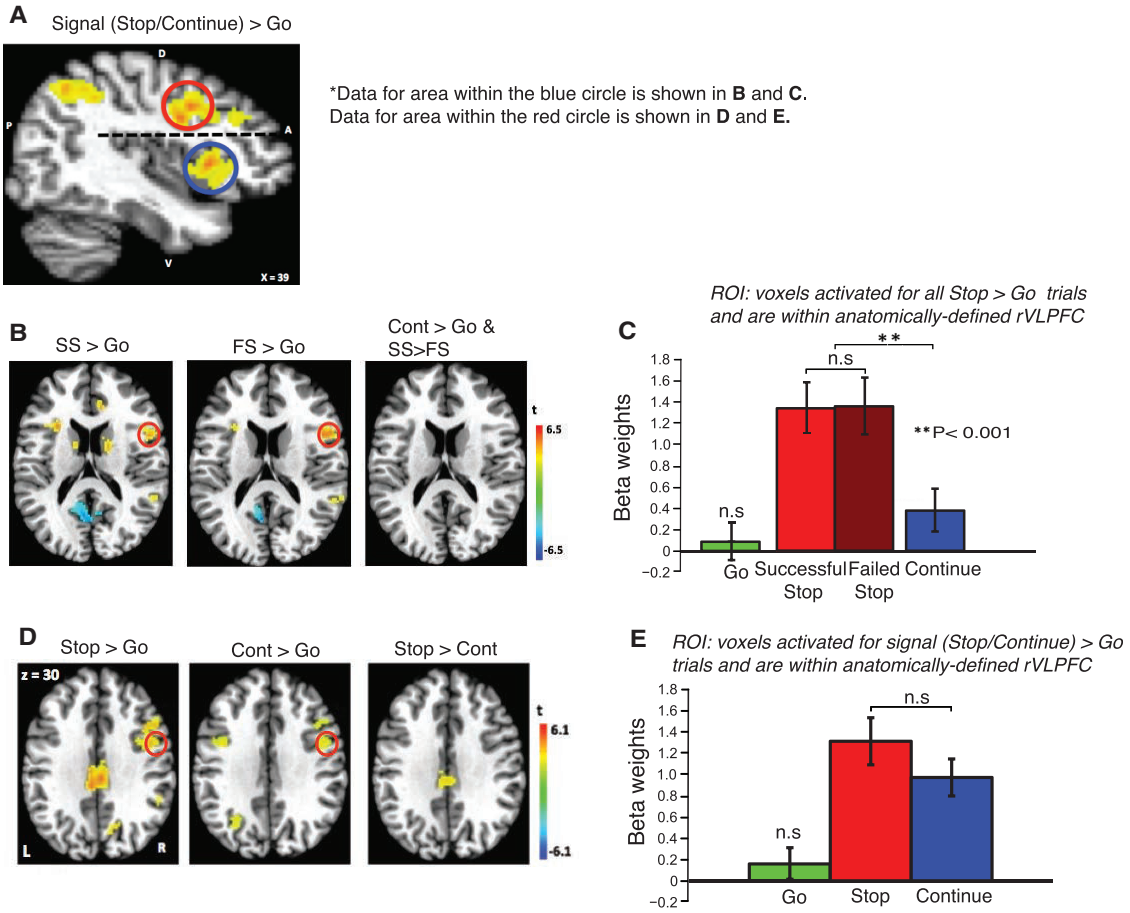

Figure 3. Human fMRI-GLM Results

(A) Areas showing greater activation (warm color) for Stop trials compared with Go trials. Red and blue circles denote the dorsal and ventral portions of the rVLPFC, respectively.

(B) Areas showing greater activation (warm colors) for Successful Stop(SS), Failed Stop(FS), and Continue trials compared with Go trials. Red circle denotes the ventral part of the rVLPFC. This region did not show greater activation for Continue trials compared to Go trials or for SS versus FS (third panel).

(C) Beta weights for Go trials (green), SS (red), FS(dark red), and Continue (blue).

(D) BOLD activation for Stop > Go, Continue > Go, and Stop > Continue. Red circle denotes the dorsal part of rVLPFC that showed elevated activity for both Stop and Continue trials.

(E) Beta weights for Go trials (green), Stop trials (red), and Continue trials (blue). The mean activations for Stop and Continue trials were statistically indistinguishable.

FEF represents Motor Output

In both dorsal and ventral regions of rVLPFC, MVPA was unable to reliably classify the pattern of BOLD activation between SS and FS trials. One possible interpretation of the results could be that the MVPA of the stop outcome was insensitive; thus, we sought to further validate the classification methods by applying the same MVPA to bilateral frontal eye field (FEF), an area known to play an important role in controlling oculomotor movement (Goldberg and Bushnell, 1981; Curtis et al., 2005; Hanes et al., 1998). We found that MVPA was able to reliably classify SS versus FS (i.e., the stop outcome) in this region (accuracy = 65% ± 5%, $t_{(20)}$ = 2.71, p = 0.013; darker gray bar for FEF in Figure 4), but not the meaning of the signal (accuracy = 57% ± 5%, $t_{(20)}$ = 1.39, p = 0.18; light gray bar for FEF in Figure 4) or the color of the signal (accuracy = 50% ± 4%, $t_{(20)}$ = 0.08, p = 0.94).

Primate Electrophysiological Results

We sought to further validate human fMRI findings by comparing the results from recording single neuron activity in rVLPFC and FEF in one macaque monkey while the animal performed a variant of the same context-based SST as in the human neuroimaging experiment (Figure 1). The primate demonstrated behavior that was similar to the human's: the Failed Stop trials yielded the shortest reaction times, and the reaction times in Continue trials were longer than in the Go trials (Figure S1). Our recording data (Figures S3–S5 showing the recording site) suggested that neurons in area 45 and 44 in the right hemisphere, a primate homolog of human rVLPFC (Petrides and Pandya 2009; Levy and Wagner, 2011), encode context information (Figures 5D–5G, 5b) and monitor trial type and response (Figure 5C, 5b). On the other hand, FEF neurons encode for movement-related activities, but not the meaning of the signal (Figures 5A

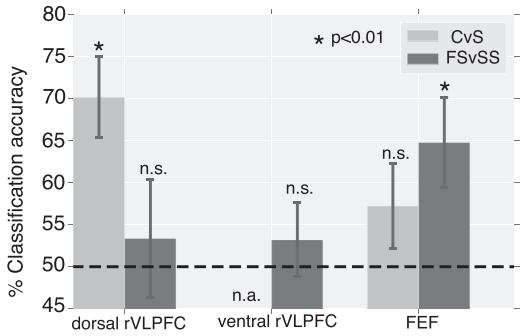

Figure 4. MVPA Classification Results

Bar graphs showing accuracies for two classification types (meaning of the signal [Continue versus Stop, light gray bar] and stop outcome [Failed Stop versus Successful Stop, darker gray bar]) across three brain regions (dorsal rVLPFC, ventral rVLPFC, and bilateral FEF). Error bar indicates SEM. Classification of Continue versus Stop in the ventral rVLPFC was not attempted because there was no significant activation in this region for Continue trials.

and 5B, 5a; Table S8 for a complete breakdown all of neuron types and counts).

FEF movement-related neurons (see Table S8) increased their firing rate when a saccade was generated (Go trials) and decreased their firing rate when a saccade was successfully inhibited (SS trials). Critically, the signal differentiation occurred before the SSRT (Figure 5A). In contrast, FEF fixation neurons decreased their firing rates for Go trials and increased their firing rates for SS trials. Again, the signal differentiation time occurred well before the SSRT, sufficient to effectively exert inhibitory control (Figure 5B). These results replicate previous findings (Hanes and Schall, 1996; Hanes et al., 1998). However, FEF neurons did not encode context-dependent information. The information contained within FEF neurons was thus consistent with the MVPA analyses of human fMRI data in this region, and the timing of these signals was shown to be sufficient to realize inhibition.

We found that some neurons in areas 44/45 preferentially increased their firing rate to a particular context. Figure 5F shows an example of a context-specific neuron that increased its firing rate to context A (red line), but not for context B (blue line). The firing rate between the two contexts remained different even after the offset of the context cue and only became equivalent at the time of the target onset. In other cases, the firing rate for the two contexts remained different long after the offset of the context cue, and even after the onset of the target, suggesting a strong preference for one context over the other (Figure 5G). These context-dependent modulations could either represent a high-level state signal or the specific behavioral rules that were associated with a particular sensory cue during this state. Thus, this neural phenomenon might represent a homolog of the task-context encoding BOLD signal shown in the human fMRI data in the dorsal rVLPFC where we found responses reflecting the context-specific meaning of the signal but not the color of the signal.

In addition, we also found area 45 neurons that increased their firing rate on switch trials, when a new context replaced the old context (Figure 5D). These neurons increased their firing rate after the onset of a new context cue on switch trials (black line in Figure 5D), but not for trials immediately after switch trials (red line) and in the middle of a block (blue line). We also found a second group of neurons in area 45 that increased firing rate gradually following a context switch (Figure 5E). These neurons increased their firing rate for switch trials (black line in Figure 5E) and continued to increase their firing rate for the trials immediately following switch trials (red line), as well as the trials in the middle of a block (blue line). These neurons indicate that this cortical area is not only responsible for encoding the currently active task set, but also controls which of multiple possible ones is selected.

Despite this strong selectivity for context, very few rVLPFC neurons encoded movement execution or inhibition. Among those that showed movement-related activities, the signal differentiation time for Go trials versus SS trials occurred after the SSRT. These rVLPFC movement-related neurons were, therefore, unable to exert inhibitory control in time to be considered causally related to the inhibition or initiation of the movement (Figures 5C and S3; see STAR Methods).

Many VLPFC neurons (60%; 197/326 cells) were systematically modulated following stop and continue signals and the behavioral response to the signal. Using a two-factor ANOVA, we distinguished seven basic response types.

The most common group was the "classifier" cells (24%; 48/197). These cells are differentially active for all three trial types. They come in two forms. One group (83%; 40/48) is most active for Failed Stop Trials, intermediately active for Continue Trials, and least active for Successful Stop Trials (Figure 6A, left). The other group (17%; 8/48) shows the inverse pattern (Figure 6A, right). The second-most-common group were the "move" cells (14%; 28/197) that were strongly active when the monkey made an eye movement (Failed Stop and Continue Trials), but not when the monkey suppressed the saccade on Successful Stop Trials (Figure 6B). The third-most-common group were the "error" cells (12%; 24/197) that responded only when the monkey made an erroneous saccade on Failed Stop Trials (Figure 6C). These cells were very similar to neurons described previously in SEF and ACC (Stuphorn et al., 2000; Ito et al., 2003). The fourth-most-common group were "stop signal" cells (6%; 11/197). These cells were only active when the monkey canceled the saccade but were too late to be responsible for the response inhibition (Figure 6D). In addition, we found two more groups in very small numbers (each 2%: 4/197). One group are the "attention" cells, which are active for all Stop and Continue Signals, independent of context (Figure 6E). They could reflect the detection of an unexpected, rare, behaviorally significant event that redirects attention. The other group are the "reward expectation" cells that are selectively active when the monkey produces the correct response and can expect reward (Figure 6F).

All of the previously described groups of neurons were characterized by a specific response to the three different trial types. Context had no effect on the vast majority of these neurons (185/197). A few showed an additive effect of context (18/197), but none of these neurons demonstrated an interactive effect

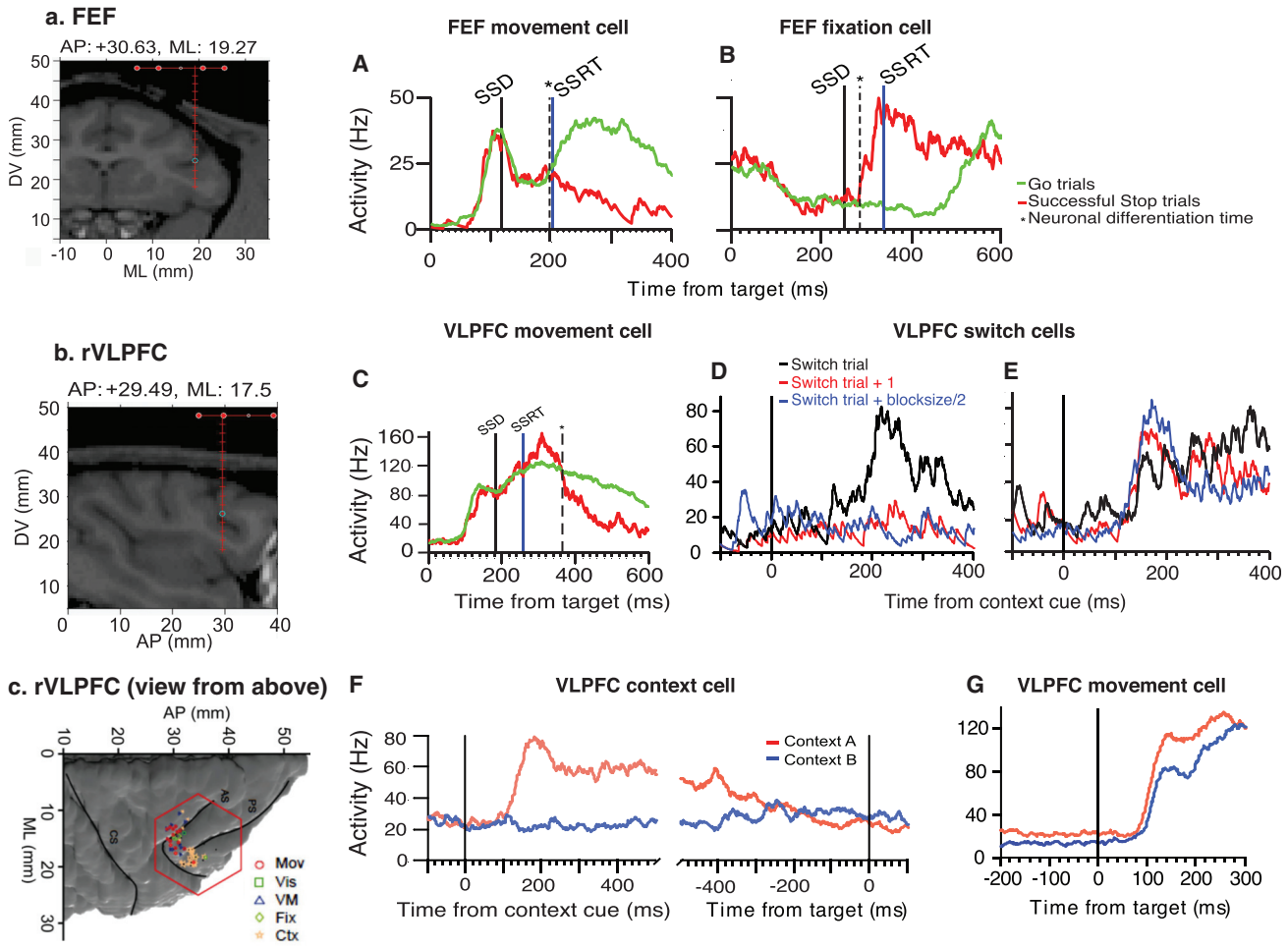

Figure 5. Primate Electrophysiology Results

Recording site (red line shows electrode penetration depth): (a) FEF; (b) rVLPFC; (c) rVLPFC dorsal surface view.

(A) A movement-related neuron in FEF increased its firing rate ~100 ms after the target onset for Go trials (green line) and decreased its firing rate for Successful Stop trials (red line). Critically, the signal differentiation time (indicated by the dashed black line) occurred before SSRT (blue solid line). Solid black line indicates the stop signal delay (SSD).

(B) A fixation neuron in FEF decreased its firing rate for Go trials and increased its firing rate for Successful Stop trials. The signal differentiation time occurred well before the SSRT.

(C) A movement-related neuron in VLPFC increased its firing rate ~120 ms after the target onset for both Go (green line) and SS (red line) trials. It then decreased its firing rate for Successful Stop trials, but the signal differentiation time (dashed black line) occurred well after SSRT (blue solid line).

(D) Activity of a VLPFC neuron increased on "context switch" trials (black line) compare to the trial immediately after switch trials (red line) and in the middle of a block (blue line).

(E) Activity of a VLPFC neuron gradually increased its firing rate in response to context cues for switch trials (black line) and continued to increase its firing rate for the trials immediately following switch trials (red line), as well as the trials in the middle of a block (blue line).

(F) A neuron increased its firing rate to context A 100 ms after the onset of the context cue (red line). In contrast, the firing rate of the same neuron remained around the baseline for context B (blue line). The firing rate between the two contexts remained different even after the offset of the context cue and only became indifferent at the time of the target onset.

(G) The firing rate of this neuron was higher for Context A (red line) than Context B (blue line) following the context cue (as in F), but this neuron also increased firing in response to the target and the difference between the contexts was even greater following the target onset.

between context and trial type. However, the response of one sizable additional group of VLPFC neurons (22%; 43/197) depended strongly on an interaction of trial type and context. These "context-switched" cells responded differentially to stop and continue signals depending on context. For example, some cells demonstrated the greatest response to Continue trials, a small response to Failed Stop trials, and suppression to Successful Stop trials, but only in Context A (when yellow = stop, Figure 6G, left). That same cell showed a large and prolonged response to Failed Stop trials, a large but briefer response to Successful Stop trials, and no response to Continue trials in Context B (when blue = stop, Figure 6G, right). The responses of these neurons are consistent with the human fMRI data in which the MVPA analysis was able to successfully classify the pattern of activity in

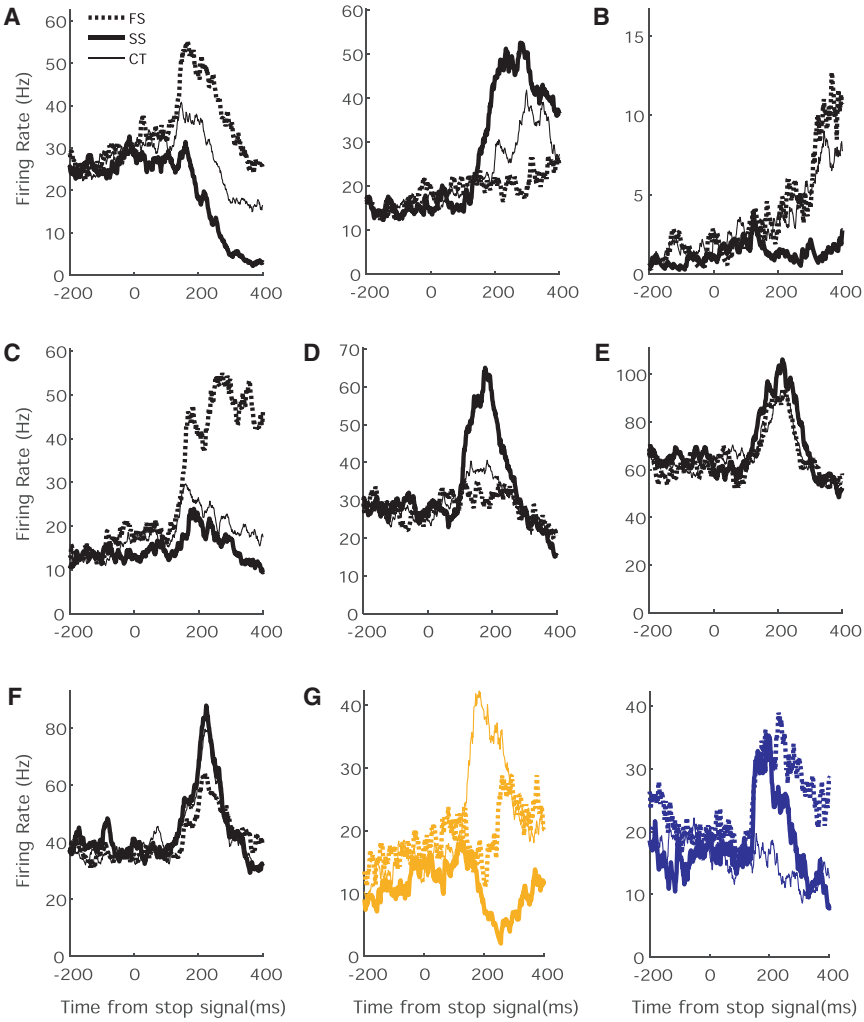

Figure 6. Neuronal Responses to Stop and Continue Signals

The activity of exemplary VLPFC neurons illustrating the seven response patterns to Stop and Continue signals. Each panel shows the activity of an individual neuron following Successful Stop signal trials (solid bold line), Failed Stop signal trials (dotted bold line), and following Continue signals (fine line). All histograms are aligned on Stop/Continue signal onset.

(A) Activity of a "classifier" cell that shows a differential activity for all three trial types. Classifier cells come in two forms. One group (shown in the left panel) is most active for Failed Stop Trials, intermediately active for Continue Trials, and least active for Successful Stop. The other group (indicated in the right panel) shows the inverse pattern.

(B) Activity of a "move" cell that is most active, when the monkey generates a saccade.

(C) Activity of an "error" cell that is most active when the monkey generates an erroneous saccade despite the presence of a stop signal.

(D) Activity of a "stop signal" cell that is most active, when the monkey successfully cancels the saccade in the presence of a stop signal.

(E) Activity of an "attention" cell that responds equally to all unexpected Stop or Continue signals.

(F) Activity of a "reward expectation" cell that responds whenever the monkey responds successfully to an unexpected event and can expect reward.

(G) Activity of a "context-switched" cell that responds differently to stop and continue signals depending on context. The two different panels show the response pattern of the same cell during context A (left, yellow = stop) and B (right, blue = stop).

dorsal rVLPFC, according to the meaning but not the color of the stimuli, indicating multiplexed coding of color and context.

Importantly, all of these responses appeared well after the SSRT/CSRT elapsed (average SSRT/CSRT: 80 ± 11 ms after stop signal onset; average neuronal response onset: 225 ± 98 ms after stop signal onset) and therefore could not cause the behavioral response to the stop or continue signals. These results, therefore, suggest that these rVLPFC movement-related neurons may have been monitoring movement rather than executing inhibitory control prior to the movement (Stuphorn et al., 2000; Ito et al., 2003).

Functional Interactions Between human rVLPFC and Other Regions Involved in Movement Control

A PPI-based analysis tests the hypothesis that activity in one brain region can be explained by an interaction between the presence of a cognitive process (i.e., psychological effect, the experimental task manipulation) and activity in another part of the brain (i.e., physiological effect; McLaren et al., 2012; Cisler et al., 2013). In the current study, we applied a PPI analysis to test the task-dependent functional connectivity (FC) among ventral rVLPFC, dorsal rVLPFC, and FEF during Go, Stop, and Continue trials and further explore the possible influence these regions may also have on other parts of the brain that were not defined *a priori*.

We found that using the dorsal part of rVLPFC as a seed region modulating Stop-related activity, significant task-dependent FC was observed in caudate and middle temporal gyrus (MTG; Figure 7A1; see Table S5 for a complete list of areas). In contrast, using the ventral part of rVLPFC as a seed region modulating Stop-related activity, significant task-dependent FC was observed with bilateral frontal eye field (FEF), left superior parietal lobule (SPL), and left putamen (Figure 7A2; Table S5).

In contrast, activity in the ventral part of rVLPFC significantly modulated Go-related activity in inferior parietal lobule (IPL), superior parietal lobe (SPL), and superior colliculus (SC) (Figure 7B1; see Table S6 for a complete list of areas). Activation in the ventral part of rVLPFC also was observed to modulate Continue-related activity in FEF, IPL, and SPL (Figure 7B2; see Table S7 for a complete list of areas). No significant modulation was observed when using the dorsal part of right VLPFC as the seed region for the Go- or Continue-related activity.

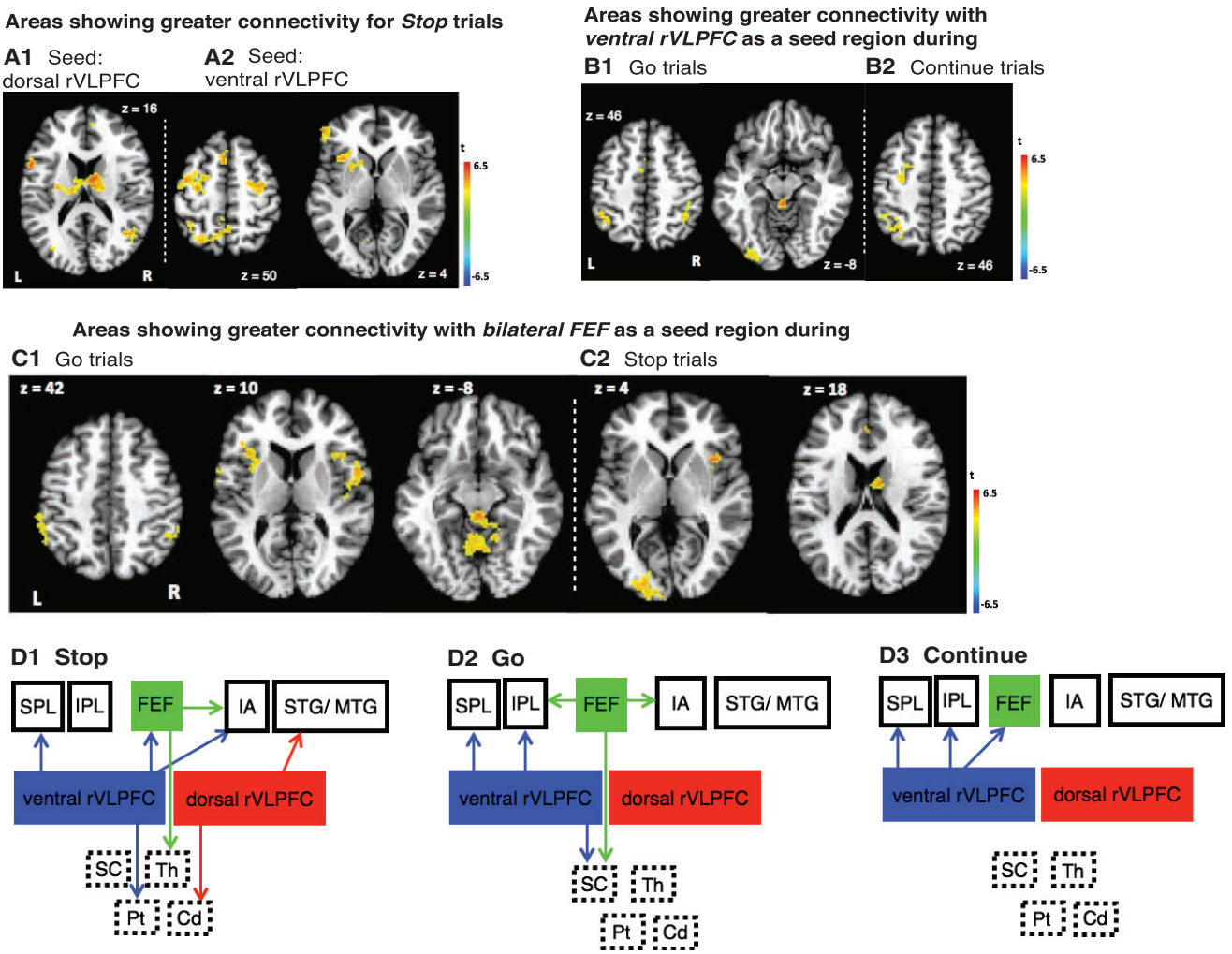

Figure 7. Human fMRI-PPI Results

Top 3 panels: areas showing greater connectivity with dorsal rVLPFC as the seed region (A1) and ventral rVLPFC as the seed region (A2) during Stop trials, compared with baseline. Areas showing greater connectivity with ventral rVLPFC as the seed region during Go trials (B1) and Continue trials (B2), compared with baseline. Areas showing greater connectivity with bilateral FEF as the seed region during Go trials (C1) and Stop trials (C2), compared with baseline. Block diagrams: summary results of functional connections among ventral rVLPFC, dorsal rVLPFC, bilateral FEF, and the rest of the brain during Stop task (D1), Go task (D2), and Continue task (D3). Solid borders indicate cortical brain regions, whereas dashed borders indicate subcortical regions. IPL, inferior parietal lobe; SPL, superior parietal lobe; FEF, frontal eye fields; IA, insula; STG: superior temporal gyrus; MTG, middle temporal gyrus; rVLPFC, right ventrolateral prefrontal cortex; SC, superior colliculus; Th, thalamus; Pt, putamen; Cd, caudate. Note: arrows do not indicate causal directionality; rather, the tail of the arrow indicates the seed region.

Furthermore, using bilateral FEF as a seed region, modulation of Go-related activity was observed in IPL, bilateral anterior insula (AI), ventral rVLPFC, and superior colliculus (SC) (Figure 7C1; Table S6). Activation in bilateral FEF was also observed to modulate Stop-related activity in left middle occipital gyrus, right AI, and right thalamus (Figure 7C2; Table S5).

DISCUSSION

Cognitive control of movement inhibition not only involves motor inhibition, but also requires attending to contextually relevant sensory information, mapping the sensory information to specific goals, and planning and executing appropriate actions. A limitation of most previous research on motor inhibition is that the "stop signal" is a perceptually salient stimulus that conflates these different processes. Building on Sharp et al. (2010), not only did we include a second "continue" stimulus to control for this attentional capture effect, but we also included a context cue that dictated the rule mapping between the two signals and their task meanings. Using fMRI, we found two functionally distinct subregions within the rVLPFC that contribute to motoric inhibition: activation in the dorsal part of the rVLPFC was associated with detecting and encoding the meaning of the signals that were behaviorally relevant, whereas the activation in the ventral part of the rVLPFC was associated with the requirement to withhold a planned eye movement, regardless of the stop outcome

(see also Erika-Florence et al., 2014). The dorsal rVLPFC in our human study roughly corresponds to BA 45B and 44, whereas the ventral part of rVLPFC roughly corresponds to BA 45A and 47 (Levy and Wagner, 2011).

Furthermore, we found that the frontal eye field (FEF), an oculomotor area controlling eye movements, encoded information regarding motor output but not the meaning of the signals or the appropriate intended behavior separate from behavioral outcome. These results replicate and extend a previous study using a different type of saccadic control task (Thakkar et al., 2014). That study also found a functional distinction between the FEF and the rVLPFC, with the FEF playing a more direct role in motor control and the rVLPFC demonstrating more activation related to inhibition, redirection, and/or attention capture. The current study design enabled a more thorough characterization of these functional distinctions. Unlike the previous study, the current study did not indicate a role for SEF in either the fMRI activation magnitude or connectivity results. This is likely due to the greater working memory demands of our context-dependent stop signal task. Previous research has shown a distinction between pre-SMA activation in a (manual) simple Go-NoGo task but DLPFC activation in a more working memory demanding Go-NoGo task (Mostofsky et al., 2003).

Primate electrophysiological recordings further validated our human fMRI results by showing that FEF neurons carried activity sufficient to control whether or not an eye movement was executed or inhibited, but not the meaning of the signals. On the other hand, neurons in area 44/45 in the right hemisphere encoded context information by either selectively increasing their firing rate to a particular context or by increasing their firing rate at the time of context switching.

This failure to identify ''inhibition-related'' activity may seem to be at odds with findings in previous monkey studies (Sakagami et al., 2001) that have been argued to be a homolog of an inhibition-specific inferior frontal cortex region (IFC) (Aron et al., 2014). However, these previous findings in monkey PFC did not support unequivocally a causal role of VLPFC in response inhibition. Most studies use a go/no-go task, in which three cognitive functions were confounded: the representation of the task rules, detection of response cues, and control of behavior (preparation or suppression of actions). It is therefore not possible to determine which specific functional signals were encoded by the neuronal activity (Sakagami et al., 2001). The same is true for another study that is often cited as evidence for a role of prefrontal cortex in inhibition, because the experimental design confounds inhibition and spatial working memory. In contrast, our experimental design explicitly distinguishes these different processes. In addition, most of these recording and stimulation studies were performed in and around the principal sulcus, but not in the area that is likely the homolog of the human IFC. The only other study in VLPFC (area 45) shows neuronal activity that distinguishes go from no-go cues but no activity during the actual execution of the go or no-go response (Sakagami et al., 2001). These results support our conclusion that VLPFC encodes context-dependent stimulus-response associations but is not directly responsible for inhibiting behavioral responses. Lastly, we do find clear inhibition-related signals, but they are located in FEF, not VLPFC.

In this context, it is an important question whether we recorded in the section of the primate prefrontal cortex that is the homolog of human rVLPFC. Our own fMRI study agrees with a recent a meta-analysis that indicates a spatially extensive right VLPFC response during response inhibition, which included portions of both pars opercularis (BA 44) and pars triangularis (BA 45) (Levy and Wagner, 2011). Cytoarchitectonic studies in macaque monkeys show a dysgranular cortical area that exhibits the characteristics of area 44 of the human brain (Petrides and Pandya, 2002, 2009; Petrides et al., 2012; Petrides, 2005). This monkey homolog of BA 44 lies anterior to ventral area 6 and is buried mostly in the most ventral part of the posterior bank and in the fundus of the inferior branch of the arcuate sulcus. Immediately rostral to this area, starting in the anterior bank of the inferior branch of the arcuate sulcus, there is another cortical area that exhibits the characteristics of area 45 of the human brain. We recorded in the anterior bank and the fundus of the arcuate sulcus (see Figures S3–S5), which represent the monkey homolog of BA 45 and partially of BA 44, corresponding to the brain region that is most likely similar to the human VLPFC region active during response inhibition. In this region, we found a large number of neurons in the monkey that were active during the stop signal task and would have resulted in a strong BOLD response.

Thus, both the primate electrophysiology and human fMRI data indicate that the rVLPFC codes for contextual information. The monkey context coding in rVLPFC was evident through both selective neural responses time locked to the context cue (which was not evident in the human BOLD fMRI activity) and in interactions between context and trial-type selective responses. In the human data, context coding was demonstrated via the context effect on the pattern of BOLD fMRI activity in response to the continue signals. The particular stimulus that indicated that a participant was to continue making the planned saccade was different in one context versus the other. Thus, in both the human and monkey data, rVLPFC contextual information appears to be multiplexed with stimulus information in order to convey stimulus meaning. The differences between monkey and human context-related activity modulations might be due to differences in recording technique. The neurons in the human rVLPFC may also respond differentially to the context cues, thus coding context independent of the stop and continue stimuli, but the BOLD fMRI signals may not have been strong enough or specific enough to detect these responses. Alternatively, there may be species differences. In addition, it is not clear whether the region in the monkey VLPFC from which we collected data in the current study corresponds to the dorsal or the ventral portion of the human VLPFC, or from both, since the border between these functionally distinct regions appears to be within area 45.

PPI analysis of human fMRI data demonstrated that dorsal rVLPFC modulated areas of the brain that are known to be part of the ''attention-breaker'' network (Corbetta and Shulman, 2002) during Stop trials, whereas ventral rVLPFC modulated areas of the brain, including FEF, that are known to be part of the goal-directed attention network and oculomotor control system (Corbetta and Shulman, 2002). Together these results suggest that the rVLPFC supports heterogeneous cognitive functions through interacting with multiple distributed networks

in the control of movement inhibition, while actual stopping is realized by the motor system through interactions with rVLPFC. This distinction between different rVLPFC regions based on functional connectivity is consistent with a previous study demonstrating distinct VLPFC regions based on anatomical connectivity in monkeys (Gerbella et al., 2010).

To control for the attentional capture effect of the Stop signal, Sharp et al. (2010) introduced Continue signal trials into the conventional SST and found that right inferior frontal gyrus (rIFG), which is equivalent to part of the rVLPFC, was active for both Stop and Continue signals, but pre-SMA was more active for Stop trials compared to Continue trials. The authors concluded that pre-SMA is associated with response inhibition, whereas rIFG is associated with attentional capture. Pre-SMA is responsible for controlling skeletomotor movement, whereas FEF is responsible for controlling eye movement. In agreement with this difference in cortical areas activated across the two studies, the Sharp et al. (2010) task involved finger button press responses while ours involved saccadic eye movements. In this regard, our BOLD activation results in FEF and rVLPFC complement the findings from the Sharp et al. (2010) study.

Importantly, our study also extended Sharp et al. (2010) by introducing a third level of control, the context manipulation, such that the meaning of a salient color stimulus was indicated by a context cue at the beginning of the trial. We found that not only was the BOLD response in dorsal rVLPFC associated with both signals' presence, but it also encoded the meaning of the signal. Thus, our findings suggest that rVLPFC encodes abstract information regarding the meaning of a particular stimulus in a given context, rather than simply sensory information *per se.*

We speculate that instead of directly exerting control over motor inhibition, the ventral part of rVLPFC is responsible for registering the intention to stop, or updating the action plan, given the current context and stimulus. Our results were not in complete agreement with Levy and Wagner's meta-analysis for the relative spatial locations among rVLPFC subregions. Our results identified two, rather than three, subregions along the dorsal-ventral axis, with dorsal rVLPFC supporting attentional orienting and task rule encoding, and ventral rVLPFC supporting stopping. This difference between the two studies could be attributed to the fact that in Levy and Wagner (2011)'s meta-analysis, the authors included Posner Cueing and Oddball tasks that particularly manipulated response uncertainty independent of response inhibition. Moreover, the large volume of studies that were included in the analysis increased the likelihood of identifying more regions showing task-related activation. Nevertheless, both studies support the argument that sub-regions within rVLPFC contribute heterogeneous functions in cognitive control of movement inhibition. These subdivisions within rVLPFC may need to be further delineated for eye versus hand movement inhibition as indicated in a previous study directly comparing the two (Leung and Cai, 2007).

One possible explanation for the above chance classification for Continue and Stop signals in dorsal rVLPFC might be that the results were driven by the differential feedback that participants received during the experiment. The mean accuracy for the Stop trials was around 50% due to task manipulation, and the average accuracy for the Continue trials was above 90%. However, if the classification results were driven by the feedback alone, then one should, by definition, be able to classify Successful Stop (SS) trials versus Failed Stop (FS) trials in this region as well. MVPA performance on classifying stop outcome in dorsal (also in ventral) rVLPFC was at chance level, which ruled out an explanation due solely to feedback processing. Furthermore, we used the frontal eye field (FEF) to benchmark the findings in rVLPFC. Our MVPA results suggested that FEF contains information regarding the stop outcome, but not the meaning of the signal. These results were consistent with existing knowledge on FEF's role in oculomotor control (Schiller et al., 1987; Bruce and Goldberg, 1985; Hanes et al., 1998; Schall and Thompson, 1999).

Corbetta and Shulman (2002) argued for two different attentional networks with one that involves preparing and applying goal-directed or "top-down" control of stimulus and response selection, and another that involves detecting behaviorally relevant stimuli with high saliency and especially when they appear unexpectedly. The authors termed this latter network the "circuit-breaking" network. The top-down control network includes part of the intraparietal sulcus (IPS) and superior frontal cortex, including the frontal eye field (FEF); the "circuit-breaking" network is mostly lateralized to the right hemisphere, which includes temporoparietal junction (TPJ) and the ventral frontal cortex (VFC), together forming the right ventral frontoparietal network (Corbetta and Shulman, 2002). Our PPI results showed that FEF and SPL were recruited through connection with ventral rVLPFC during Go and Stop tasks to exert control of eye movements—either to initiate or inhibit a saccade. In addition, dorsal rVLPFC was functionally connected with superior temporal gyrus (STG) and MTG during Stop trials, presumably because the Stop signal was behaviorally relevant, with a high visual saliency and appeared unexpectedly. In this sense, the dorsal rVLPFC, STG, and MTG served as a ventral attentional circuit-breaker to interrupt goal-directed attentional control during stopping.

Erika-Florence et al. (2014) found that rVLPFC subregions were not functionally unique in their sensitivities to inhibitory control but instead formed distributed networks that were active when infrequent stimuli appeared, regardless of whether inhibitory control was needed, or whenever novel stimuli appeared that led to new response adjustment as opposed to predictable or routine responses. The authors thus concluded that there is no specific module in the prefrontal cortex that is dedicated to inhibitory control, but rather, response inhibition is an emergent property of a distributed network in the brain that instantiates cognitive control (Erika-Florence et al., 2014). A similar conclusion was drawn by Verbruggen et al. (2010), who found that transcranial magnetic stimulation to a ventral portion of rVLPFC disrupted both stopping behavior and dual-task performance.

There is evidence in our study that further supports these interpretations of the role of rVLPFC in inhibitory control. We found that ventral rVLPFC was functionally connected with the putamen while the dorsal rVLPFC was functionally connected with the caudate during stop-related processes, suggesting a potential cognitive versus motor functional dissociation. Second, ventral rVLPFC is connected with SC during Go trials, suggesting

a role in reflexive, expected motor execution, not just in inhibitory motor control. Furthermore, ventral rVLPFC modulated FEF activity not only during Stop trials but also during Continue trials. These results support the idea that ventral and dorsal rVLPFC are functionally distinct parts of a set of distributed networks that broadly underlies cognitive control, rather than response inhibition specifically.

In conclusion, our findings indicate multiple brain areas involved in multiple complex and task-dependent circuits, all of which contribute to context-dependent and stimulus-selective control of behavior. Within this complex network, the role of VLPFC seems to be the encoding of context-specific task rules and the detection or monitoring of the need for response inhibition, but not its initiation or instantiation.

STAR★METHODS

Detailed methods are provided in the online version of this paper and include the following:

- KEY RESOURCES TABLE
- CONTACT FOR REAGENT AND RESOURCE SHARING
- EXPERIMENTAL MODEL AND SUBJECT DETAILS
  - Human fMRI experiment
  - Primate electrophysiology experiment
- METHOD DETAILS
  - Human fMRI experiment
  - Primate electrophysiology experiment
- QUANTIFICATION AND STATISTICAL ANALYSIS
  - Human fMRI experiment
  - Primate electrophysiology experiment
- DATA AND SOFTWARE AVAILABILITY

SUPPLEMENTAL INFORMATION

Supplemental Information includes five figures and eight tables and can be found with this article online at https://doi.org/10.1016/j.neuron.2017.11.010.

AUTHOR CONTRIBUTIONS

K.Z.X. helped design the experiments, collected fMRI and electrophysiological data, analyzed data, and wrote the manuscript. B.A.A. and A.W.S. helped with fMRI data analysis and editing the manuscript. V.S. helped design the experiments. E.E.E. and V.S. helped with electrophysiology data collection and analysis and with editing the manuscript. S.Y. helped design the experiments and with fMRI data collection. S.M.C. helped with fMRI data analysis, interpretation and comparison across human and monkey experiments, and editing the manuscript.

ACKNOWLEDGMENTS

The authors thank the entire staff of the F.M. Kirby Research Center for Functional Brain Imaging where the fMRI data were collected. This work was supported by grants from the National Institute in Drug Abuse R01-DA013165 to S.Y. and S.M.C., from the National Institute of Neurological Disorders and Stroke (NINDS) R01NS086104, and the National Institute on Drug Abuse (NIDA) RO1DA040990 to V.S.

Received: March 18, 2017
Revised: July 21, 2017
Accepted: November 8, 2017
Published: December 7, 2017

REFERENCES

Aron, A.R., Fletcher, P.C., Bullmore, E.T., Sahakian, B.J., and Robbins, T.W. (2003). Stop-signal inhibition disrupted by damage to right inferior frontal gyrus in humans. Nat. Neurosci. *6*, 115–116.

Aron, A.R., Robbins, T.W., and Poldrack, R.A. (2014). Right inferior frontal cortex: addressing the rebuttals. Front. Hum. Neurosci *8*, 905.

Asaad, W.F., and Eskandar, E.N. (2008). A flexible software tool for temporally-precise behavioral control in Matlab. J. Neurosci. Methods *174*, 245–258.

Botvinick, M.M., Braver, T.S., Barch, D.M., Carter, C.S., and Cohen, J.D. (2001). Conflict monitoring and cognitive control. Psychol. Rev. *108*, 624–652.

Botvinick, M.M., Cohen, J.D., and Carter, C.S. (2004). Conflict monitoring and anterior cingulate cortex: an update. Trends Cogn. Sci. *8*, 539–546.

Bradley, A., Skottun, B.C., Ohzawa, I., Sclar, G., and Freeman, R.D. (1987). Visual orientation and spatial frequency discrimination: a comparison of single neurons and behavior. J. Neurophysiol. *57*, 755–772.

Britten, K.H., Shadlen, M.N., Newsome, W.T., and Movshon, J.A. (1992). The analysis of visual motion: a comparison of neuronal and psychophysical performance. J. Neurosci. *12*, 4745–4765.

Brown, J.W., Hanes, D.P., Schall, J.D., and Stuphorn, V. (2008). Relation of frontal eye field activity to saccade initiation during a countermanding task. Exp. Brain Res. *190*, 135–151.

Bruce, C.J., and Goldberg, M.E. (1985). Primate frontal eye fields. I. Single neurons discharging before saccades. J. Neurophysiol. *53*, 603–635.

Chang, C.C., and Lin, C.J. (2001). LIBSVM: A Library for Support Vector Machines (Online). http://www.csie.ntu.edu.tw/_cjlin/libsvm.

Chikazoe, J., Jimura, K., Asari, T., Yamashita, K., Morimoto, H., Hirose, S., Miyashita, Y., and Konishi, S. (2009). Functional dissociation in right inferior frontal cortex during performance of go/no-go task. Cereb. Cortex *19*, 146–152.

Cisler, J.M., Bush, K., and Steele, J.S. (2013). A comparison of statistical methods for detecting context-modulated functional connectivity in fMRI. NeuroImage *84*, 1042–1052.

Connolly, J.D., Goodale, M.A., Goltz, H.C., and Munoz, D.P. (2005). fMRI activation in the human frontal eye field is correlated with saccadic reaction time. J. Neurophysiol. *94*, 605–611.

Corbetta, M., and Shulman, G.L. (2002). Control of goal-directed and stimulus-driven attention in the brain. Nat. Rev. Neurosci. *3*, 201–215.

Courtney, S.M., Ungerleider, L.G., Keil, K., and Haxby, J.V. (1996). Object and spatial visual working memory activate separate neural systems in human cortex. Cereb. Cortex *6*, 39–49.

Cox, R.W. (1996). AFNI: software for analysis and visualization of functional magnetic resonance neuroimages. Comput. Biomed. Res. *29*, 162–173.

Curtis, C.E., Cole, M.W., Rao, V.Y., and D'Esposito, M. (2005). Canceling planned action: an FMRI study of countermanding saccades. Cereb. Cortex *15*, 1281–1289.

Egan, J.P. (1975). Signal Detection Theory and ROC Analysis (Academic Press).

Erika-Florence, M., Leech, R., and Hampshire, A. (2014). A functional network perspective on response inhibition and attentional control. Nat. Commun. *5*, 4073.

Gerbella, M., Belmalih, A., Borra, E., Rozzi, S., and Luppino, G. (2010). Cortical connections of the macaque caudal ventrolateral prefrontal areas 45A and 45B. Cereb. Cortex *20*, 141–168.

Goldberg, M.E., and Bushnell, M.C. (1981). Behavioral enhancement of visual responses in monkey cerebral cortex. II. Modulation in frontal eye fields specifically related to saccades. J. Neurophysiol. *46*, 773–787.

Green, D.M., and Swets, J.A. (1966). Signal Detection Theory and Psychophysics, *Volume 1* (New York Press), p. 521.

Guido, W., Lu, S.M., Vaughan, J.W., Godwin, D.W., and Sherman, S.M. (1995). Receiver operating characteristic (ROC) analysis of neurons in the cat's lateral

geniculate nucleus during tonic and burst response mode. Vis. Neurosci. *12*, 723–741.

Hanes, D.P., and Schall, J.D. (1996). Neural control of voluntary movement initiation. Science *274*, 427–430.

Hanes, D.P., Patterson, W.F., 2nd, and Schall, J.D. (1998). Role of frontal eye fields in countermanding saccades: visual, movement, and fixation activity. J. Neurophysiol. *79*, 817–834.

Hanke, M., Halchenko, Y.O., Sederberg, P.B., Hanson, S.J., Haxby, J.V., and Pollmann, S. (2009). PyMVPA: A python toolbox for multivariate pattern analysis of fMRI data. Neuroinformatics *7*, 37–53.

Ito, S., Stuphorn, V., Brown, J.W., and Schall, J.D. (2003). Performance monitoring by the anterior cingulate cortex during saccade countermanding. Science *302*, 120–122.

Jenkinson, M., Beckmann, C.F., Behrens, T.E., Woolrich, M.W., and Smith, S.M. (2012). FSL. Neuroimage *62*, 782–790.

Koechlin, E., Ody, C., and Kouneiher, F. (2003). The architecture of cognitive control in the human prefrontal cortex. Science *302*, 1181–1185.

Leung, H.C., and Cai, W. (2007). Common and differential ventrolateral prefrontal activity during inhibition of hand and eye movements. J. Neurosci. *27*, 9893–9900.

Levy, B.J., and Wagner, A.D. (2011). Cognitive control and right ventrolateral prefrontal cortex: reflexive reorienting, motor inhibition, and action updating. Ann. N Y Acad. Sci. *1224*, 40–62.

Logan, G.D., Cowan, W.B., and Davis, K.A. (1984). On the ability to inhibit simple and choice reaction time responses: a model and a method. J. Exp. Psychol. Hum. Percept. Perform. *10*, 276–291.

Macmillan, N.A., and Creelman, C.D. (2004). Detection Theory: A User's Guide (Psychology Press).

Mayse, J.D., Nelson, G.M., Park, P., Gallagher, M., and Lin, S.-C. (2014). Proactive and reactive inhibitory control in rats. Front. Neurosci. *8*, 104.

McLaren, D.G., Ries, M.L., Xu, G., and Johnson, S.C. (2012). A generalized form of context-dependent psychophysiological interactions (gPPI): a comparison to standard approaches. Neuroimage *61*, 1277–1286.

Mostofsky, S.H., Schafer, J.G., Abrams, M.T., Goldberg, M.C., Flower, A.A., Boyce, A., Courtney, S.M., Calhoun, V.D., Kraut, M.A., Denckla, M.B., and Pekar, J.J. (2003). fMRI evidence that the neural basis of response inhibition is task-dependent. Brain Res. Cogn. Brain Res. *17*, 419–430.

Norman, K.A., Polyn, S.M., Detre, G.J., and Haxby, J.V. (2006). Beyond mind-reading: multi-voxel pattern analysis of fMRI data. Trends Cogn. Sci. *10*, 424–430.

Paré, M., and Hanes, D.P. (2003). Controlled movement processing: superior colliculus activity associated with countermanded saccades. J. Neurosci. *23*, 6480–9.

Petrides, M. (2005). Lateral prefrontal cortex: architectonic and functional organization. Philos. Trans. R. Soc. Lond. B Biol. Sci. *360*, 781–795.

Petrides, M., and Pandya, D.N. (2002). Comparative cytoarchitectonic analysis of the human and the macaque ventrolateral prefrontal cortex and corticocortical connection patterns in the monkey. Eur. J. Neurosci. *16*, 291–310.

Petrides, M., and Pandya, D.N. (2009). Distinct parietal and temporal pathways to the homologues of Broca's area in the monkey. PLoS Biol. *7*, e1000170.

Petrides, M., Tomaiuolo, F., Yeterian, E.H., and Pandya, D.N. (2012). The prefrontal cortex: comparative architectonic organization in the human and the macaque monkey brains. Cortex *48*, 46–57.

Sakagami, M., Tsutsui, K., Lauwereyns, J., Koizumi, M., Kobayashi, S., and Hikosaka, O. (2001). A code for behavioral inhibition on the basis of color, but not motion, in ventrolateral prefrontal cortex of macaque monkey. J. Neurosci. *21*, 4801–4808.

Sayer, R.J., Friedlander, M.J., and Redman, S.J. (1990). The time course and amplitude of EPSPs evoked at synapses between pairs of CA3/CA1 neurons in the hippocampal slice. J. Neurosci. *10*, 826–836.

Schall, J.D., and Thompson, K.G. (1999). Neural selection and control of visually guided eye movements. Annu. Rev. Neurosci. *22*, 241–259.

Schiller, P.H., Sandell, J.H., and Maunsell, J.H. (1987). The effect of frontal eye field and superior colliculus lesions on saccadic latencies in the rhesus monkey. J. Neurophysiol. *57*, 1033–1049.

Sebastian, A., Jung, P., Neuhoff, J., Wibral, M., Fox, P.T., Lieb, K., Fries, P., Eickhoff, S.B., Tüscher, O., and Mobascher, A. (2016). Dissociable attentional and inhibitory networks of dorsal and ventral areas of the right inferior frontal cortex: a combined task-specific and coordinate-based meta-analytic fMRI study. Brain Struct. Funct. *221*, 1635–1651.

Serences, J.T., Schwarzbach, J., Courtney, S.M., Golay, X., and Yantis, S. (2004). Control of object-based attention in human cortex. Cereb. Cortex *14*, 1346–1357.

Serences, J.T., Shomstein, S., Leber, A.B., Golay, X., Egeth, H.E., and Yantis, S. (2005). Coordination of voluntary and stimulus-driven attentional control in human cortex. Psychol. Sci. *16*, 114–122.

Sharp, D.J., Bonnelle, V., De Boissezon, X., Beckmann, C.F., James, S.G., Patel, M.C., and Mehta, M.A. (2010). Distinct frontal systems for response inhibition, attentional capture, and error processing. Proc. Natl. Acad. Sci. USA *107*, 6106–6111.

Stuphorn, V., Taylor, T.L., and Schall, J.D. (2000). Performance monitoring by the supplementary eye field. Nature *408*, 857–860.

Talairach, J., and Tournoux, P. (1988). Co-planar Stereotaxic Atlas of the Human Brain (Thieme Medical Publishers).

Thakkar, K.N., van den Heiligenberg, F.M., Kahn, R.S., and Neggers, S.F. (2014). Frontal-subcortical circuits involved in reactive control and monitoring of gaze. J. Neurosci. *34*, 8918–8929.

Tolhurst, D.J., Movshon, J.A., and Dean, A.F. (1983). The statistical reliability of signals in single neurons in cat and monkey visual cortex. Vision Res. *23*, 775–785.

Verbruggen, F., Aron, A.R., Stevens, M.A., and Chambers, C.D. (2010). Theta burst stimulation dissociates attention and action updating in human inferior frontal cortex. Proc. Natl. Acad. Sci. USA *107*, 13966–13971.

Vogels, R., and Orban, G.A. (1990). How well do response changes of striate neurons signal differences in orientation: a study in the discriminating monkey. J. Neurosci. *10*, 3543–3558.

Xu, K.Z. (2016). Neural basis of cognitive control of movement inhibition. Dissertation (Johns Hopkins University). http://jhir.library.jhu.edu/handle/1774.2/40270.

Yantis, S. (1993). Stimulus-driven attentional capture and attentional control settings. J. Exp. Psychol. Hum. Percept. Perform. *19*, 676–681.

Yantis, S., and Jonides, J. (1990). Abrupt visual onsets and selective attention: voluntary versus automatic allocation. J. Exp. Psychol. Hum. Percept. Perform. *16*, 121–134.

Zohary, E., Hillman, P., and Hochstein, S. (1990). Time course of perceptual discrimination and single neuron reliability. Biol. Cybern. *62*, 475–486.

STAR★METHODS

KEY RESOURCES TABLE

REAGENT or RESOURCE	SOURCE	IDENTIFIER
Deposited Data		
Raw data	human fMRI data: Susan Courtney (courtney@jhu.edu). monkey electrophysiological data: Veit Stuphorn (veit@jhu.edu)	N/A
Experimental Models: Organisms/Strains		
Maccaca mulatta	Johns Hopkins University	N/A
Software and Algorithms		
Modified integration method for estimating SSRT/CSRT	This paper; Mayse et al., 2014	N/A

CONTACT FOR REAGENT AND RESOURCE SHARING

As Lead Contact, Susan Courtney is responsible for all reagent and resource requests. Please contact Susan Courtney at courtney@jhu.edu with requests and inquiries.

EXPERIMENTAL MODEL AND SUBJECT DETAILS

Human fMRI experiment

Participants

21 participants (7 M, 14 F, mean age of 22 (range, 18-30 years)) were recruited from the Johns Hopkins community. All were screened for normal or corrected-to-normal visual acuity and color vision. Written, informed consent was obtained from all participants, and all of the experimental procedures were approved by the Institutional Review Boards of the Johns Hopkins University and the Johns Hopkins Medical Institutions.

Procedure

All participants completed either 4 or 5, 1.5-hour behavioral training sessions and one 1.75-hour fMRI scanning session with a context-dependent stop signal task, in exchange for monetary compensation. All participants' last two behavioral training sessions met *a priori* criteria for them to be qualified for the fMRI scanning session. The criteria were set such that the average performance accuracy was no less than 40% for Stop trials and 80% for Continue trials. This was to ensure that participants were performing Stop and Continue tasks as instructed.

Primate electrophysiology experiment

We acquired single unit activity from 55 neurons in frontal eye field (FEF) and 326 neurons in area 45, which is located anterior to the inferior spur of the arcuate sulcus in macaque monkeys (Table S8). Evidence from comparative neuroanatomical studies suggests that area 45 is the macaque homolog of the human VLPFC (Petrides and Pandya, 2009).

METHOD DETAILS

Human fMRI experiment

Apparatus and stimuli

A Mac computer (Apple, Cupertino, California, USA) equipped with MATLAB software (https://www.mathworks.com/) and PsychToolbox-3 extensions (http://psychtoolbox.org/) was used to present the stimuli. During the behavioral training sessions, participants viewed an Asus LED HD monitor (60 Hz refresh rate), from a distance of ~56 cm in a dimly lit room. Eye positions were sampled from the right eye and recorded with an infrared corneal reflection system, EyeLink 1000 (SR Research, Mississauga, Ontario, Canada) at a sampling rate of 500 Hz. During the fMRI scanning sessions, eye position was sampled from the right eye and recorded with an infrared corneal reflection system, EyeLink 1000 Plus (SR Research, Mississauga, Ontario, Canada), located at the back of the bore of the scanner, at a sampling rate of 500 Hz. All stimuli were displayed on a back-projected screen located in the bore of the scanner, which participants viewed through a mirror attached to the head coil. For both behavioral training and fMRI scanning sessions, five-point calibrations were performed at the beginning of the session and between each run. Saccadic eye movements

were detected online using the EyeLink built-in algorithm in order to give participants performance feedback during the experiment. A valid saccade was further admitted to the behavioral analysis offline if it started from the central fixation window (3° x 3°, visual angle) and ended in the peripheral target window (3° x 3°).

Stimuli included a shape context cue, a central fixation point, a target, a colored stop signal, and a colored continue signal. All stimuli were 1° x 1° in size, and were presented against a gray background. The target stimuli were presented at an eccentricity of 10° horizontally from the fixation point, either to the left or to the right.

Procedure

Each participant received 3 types of trials: Go trials, Stop trials, and Continue trials, presented in a pseudo-randomized order (Figure 1). All trials started when participants acquired central fixation at a context cue. The shape of the context cue (square or triangle) indicated the rule mapping on that trial, and was visible for 500 ms before it was replaced by a central fixation point. After a random delay (2000ms + jitter; jitter varied from 0 to 1500ms, incrementing by 500ms) the fixation point was then extinguished and, simultaneously, a peripheral target appeared. On Go trials, the target appeared alone and a trial was considered correct if participants generated a single saccade to the target (+/− 2.5° offset) within the 500ms maximum response time window and maintained their gaze at the target for an additional 200ms. On Stop and Continue trials, a central stimulus (blue or yellow dot) was presented after a variable delay (stop signal delay, SSD, for Stop trials, and continue signal delay, CSD, for Continue trials) following the target onset. On Stop trials, the trial was correct if participants maintained fixation for 400ms after the stop signal was presented, indicating that they had canceled the preparation of their planned saccade. On Continue trials, the trial was correct if participants successfully generated a saccade to the target, despite the presentation of a continue signal. Four fixed SSDs were selected empirically based on each individual's performance during the behavioral training sessions such that at the shortest SSD, participants generally inhibited the movement in > 75% of the Stop trials and at the longest delay, participants inhibited the movement in < 25% of the Stop trials, and most of the data points were centered around the two SSDs in which the participants inhibited the movement on ~50% of the Stop trials. The SSDs ranged between 50 ms to 250 ms. The same delays were used for Continue trials for the same participant and were referred to as continue signal delays (CSDs). In one context, a yellow dot cued the participants to cancel the saccade (Stop trials) while a blue dot cued the participants to ignore it and make a saccade to the peripheral target (Continue trials). In the other context, the rule was reversed. Three inter-trial intervals (ITIs), 2 s, 4 s, and 6 s, were used and were pseudo-randomly determined resulting in 60%, 30%, and 10% of trials, respectively. The context alternated every 8, 10 or 16 trials, randomly and without prior warning. The first trial following the context alternation was termed a "switch" trial.

fMRI Data Collection

MR images were acquired with a Phillips Intera 3T scanner at the Kirby Center for Functional Brain Imaging at the Kennedy Krieger Institute in Baltimore, MD. For each participant, a high-resolution anatomical scan was acquired with an MPRAGE T1-weighted sequence with an isotropic voxel size of 1 mm [repetition time (TR) = 8.1 ms; echo time (TE) = 3.7 ms, flip angle = 8°, 150 axial slices, 0 mm gap, SENSE factor = 2]. Whole-brain, T2*-weighted echo-planar images were acquired with a 32-channel SENSE headcoil in 36 transverse, sequential slices [TR = 2000ms, TE = 30 ms; flip angle = 70°, acquisition matric = 76 x76, field of view = 192.00mm x 171.79mm x 107.50mm; slice thickness 2.5 mm, gap = 0.5 mm; SENSE factor = 2], yielding voxels that were 2.5mm isotropic.

Each EPI scan began with 4 dummy pulses in order to allow magnetization to reach steady-state. We acquired 234 volumes for each of the 6 experimental runs such that each lasted approximate 7.8 minutes.

Preprocessing of the data was carried out in AFNI (Cox, 1996) with the exception of removing the skull from the anatomical scan, which was carried out using fsl_anat (Jenkinson et al., 2012). We applied AFNI's nonlinear warping (3dQWarp) to morph each participant's anatomical scan into Talairach stereotaxic space (Talairach and Tournoux, 1988) according to the Colin 27 template. All functional images were first corrected for slice time acquisition. Next, we corrected for participant motion and registered each image to the corresponding normalized anatomical image. The functional runs were resampled to an isotropic resolution of 2mm during coregistration. Lastly, we performed spatial smoothing with a kernel of 4 mm full width half maximum and normalized the BOLD response in each voxel to the voxel's average MR signal magnitude across the six experimental runs.

Primate electrophysiology experiment

Subject and general task set-up

One rhesus macaque monkey was trained to perform a visually guided saccade task and a context-dependent SST by operant conditioning with positive reinforcement. All animal care and experimental procedures were approved by The Johns Hopkins University Animal Care and Use Committee. Monkeylogic software (http://www.brown.edu/Research/monkeylogic/) (Asaad and Eskandar, 2008) was used to control task events, stimuli and rewards, and to monitor and store behavioral events. During the experimental sessions, the monkey was seated in a primate chair, with its head restrained, facing a video monitor. Eye positions were monitored and recorded with an infrared corneal reflection system, EyeLink 1000 (SR Research) at a sampling rate of 1000 Hz. Eye movements were detected offline using a computer algorithm that searched first for significantly elevated velocity (30°/s). Saccade initiation and termination then were defined as the beginning and end of the monotonic change in eye position lasting 15 ms before and after the high-velocity gaze shift. A valid saccade was further admitted to the behavioral analysis if it started from the central fixation window (2.5°x 2.5°) and ended in the peripheral target window (2.5°x 2.5°). Visual inspection was also applied to ensure the accuracy of saccade detection.

Behavioral task

The context-dependent SST was run after a neuron's response field was successfully mapped out by the visually guided saccade task. The context-dependent SST was very similar to the one used in the human fMRI study, except that a trial started with the monkey acquiring central fixation on a white dot, which was then replaced by a shaped context cue. The timing of the stimuli onset was adjusted for the electrophysiology experiment as well (Figure 1). Five fixed Stop signal delays (SSD) ranging from 100ms to 300ms, with a 50ms increment, were used such that at the shortest Stop signal delay, monkeys generally inhibited the movement in > 75% of the Stop trials and at the longest delay, monkeys inhibited the movement in < 25% of the Stop trials, and most of the data points were centered around the SSD in which the monkey inhibited the movement in 50% of the Stop trials. The Continue signal delay (CSD) had the identical timing as the SSD. The monkey generally inhibited the movement in < 5% of the Continue trials, for all CSD.

The context-based stop signal task was run in a block fashion. Within each block, only one type of context cue, either a square-shaped cue or a triangle-shaped cue, was shown to the monkey. Each block contained either 50 or 100 trials, and alternated between square-cue block and triangle-cue block such that the two types of blocks were counterbalanced. The first trial of a new block was coined a "switch" trial.

Cortical localization

We used T1 and T2 magnetic resonance images (MRIs) obtained for the monkey (3.0 T) to determine the location of the area 45 and FEF. Anatomically, area 45 is located in the midline, 12mm anterior to the inferior spur of the arcuate sulcus, extending to the principle sulcus. FEF is located in the fundus of the arcuate sulcus, more posterior and medial relative to area 45.

Single-unit recording

After training, we surgically placed a recording chamber centered over area 45 and FEF on the right hemisphere of the animal. Single units were recorded using tungsten microelectrodes (2–4 MΩ) that were under the control of a microdrive. Electrodes were inserted through a guide tube positioned and lowered to just above the surface of the dura mater. Electrophysiological data were collected using the TDT system (Tucker & Davis) at a sampling rate of 1-kHz. Action potentials were amplified, filtered, and discriminated conventionally with a time-amplitude window discriminator. Spikes were isolated online if the amplitude of the action potential was sufficiently above background to reliably trigger the time-amplitude window discriminator, the waveform of the action potential was invariant throughout experimental recording, and the isolation could be sustained for sufficient period of recording. The identification and isolation of individual spikes was reevaluated and corrected offline using three-dimensional PCA and visual inspection of selected waveforms (Offline Sorter Program, Plexon .Inc) to ensure only single units were included in subsequent data analysis.

QUANTIFICATION AND STATISTICAL ANALYSIS

Human fMRI experiment

Behavioral Data and Estimation of SSRT/CSRT

All behavioral data were analyzed using custom-written MATLAB (https://www.mathworks.com) scripts. Reaction times (RTs) were calculated as the time between go signal onset and the initiation of a saccade, and were expressed as mean ± 1 s.e.m. Inhibition functions were constructed by fitting a Weibull function to the relationship between the stop signal delay and the proportion of Failed Stop trials over all Stop trials (i.e., the probability of generating a saccade over all Stop trials).

To estimate SSRT and CSRT we used the modified integration method. This method has been described in detail previously and this description is summarized here (Mayse et al., 2014). This method is computationally similar to the integration method, in which SSRT is determined by finding the point on the Go RT distribution at which the area-under-the-curve equals the proportion of Failed Stop trials for a given SSD, then aligning this point to the stop signal by subtracting SSD from Go RT. SSRT is then determined by averaging these SSRTs across all SSDs. The modified integration method allows for estimation of SSRT and CSRT by comparing the signal distribution (either continue or stop) to a yoked go trial RT distribution (the go RT distribution aligned to the stop signal). See Figure S2. See also Xu (2016). This method was implemented in the following steps: First, we drew *n* (where *n* is the number of stop or continue trials) random samples without replacement from the number of Go trials in a session. These RTs were aligned to the stop signal by subtracting from this sampling distribution the actual *n* SSDs or CSDs. Separate, yoked Go RT distributions were created for estimation of SSRT and CSRT. Second, this sampling and aligning procedure was repeated 10,000 times to construct a 99.9% (0.05%–99.95%) confidence interval (CI) of the yoked Go RT distribution. Third, we determined the first time point in the sorted Stop or Continue trial RT distribution that fell outside the 99.9% CI (this time point was calculated as the first time point at which at least 0.15*n* consecutive stop or continue trials were greater than the upper bound of the 99.9% CI to protect against false positives in noisy cumulative RT distributions). This time point is not SSRT or CSRT (which is a point on the Stop or Continue trial RT distribution, not the 99.9% CI) but was used as a conservative cutoff to separate fast and slow continue trials (Mayse et al., 2014). Finally, using this cutoff value, we were able to find the proportion of failed stop or fast continue trials. We then estimated SSRT (CSRT) by finding the latency relative to the Stop (Continue) signal at which the density of the cumulative distribution of Stop-aligned Stop trial (Continue-aligned Continue trial) RTs was equal to the proportion of Failed Stop (Fast Continue) trials. It has been previously demonstrated that SSRTs derived using this method are indistinguishable from SSRTs derived using the integration or median methods (Mayse et al., 2014).

fMRI Univariate analysis

We used a voxelwise general linear model for testing the main effect of motor inhibition and/or reflexive reorienting attention to external events. Task-dependent changes in BOLD signal were modeled to test whether elevated BOLD activity in rVLPFC was correlated with motor inhibition and/or with reflexive reorienting of attention to external events, using separate regressors representing each possible combination of the two signal colors (blue or yellow) and five trial outcomes (Correct Go, Successful Stop, Failed Stop, Slow Continue, and Fast Continue). Each regressor was time-locked to the target onset. In addition, six head-motion parameters were included in the model as regressors-of-non-interest. All regressors were convolved with a canonical hemodynamic response function (HRF) using a double gamma function. Contrasts of interest were created for each participant to identify voxels exhibiting greater BOLD responses on: 1) Successful Stop (SS) trials compared with Go trials, 2) Failed Stop (FS) trials compared with Go trials, 3) SS trials compared with FS trials, 4) Stop (SS +FS) trials compared with Go trials, regardless of the outcome of the stopping, 5) Continue trials compared with Go trials, and 6) Stop trials compared with Continue trials. All contrasts created at the participant-level were entered into a group-level random-effect analysis using a one-sample t test against a contrast value of zero at each voxel. The statistical maps were thresholded using a voxel-level threshold of $p < 0.01$, corrected for multiple comparisons at a cluster-level of $p < 0.05$ (family-wise error correction). All whole-brain group-level results were corrected for multiple comparisons by running 10,000 Monte Carlo simulations in 3dClustSim to determine the probability of obtaining a cluster of significant activity of a certain size given the spatial smoothness of the data.

Defining Regions of Interest for testing motor inhibition

We first used the Stop > Go contrast in the group-level GLM analysis to identify right lateral prefrontal regions that showed significant activation. Next, we manually created an anatomical "mask" for right inferior frontal gyrus (rIFG) using AFNI built-in N27 brain Atlas. (AFNI atlas uses IFG to designate VLPFC). Regions of interest (ROI) were defined as the overlapping area between the functionally defined lateral prefrontal regions and the anatomical mask of rIFG. We extracted the beta weights of the ROI, averaged across all voxels in the ROI, for each participant for the following three regressors/contrasts: 1) Go trials - baseline, 2) SS - Go trials, 3) FS - Go trials. Positive value indicates greater BOLD activity.

Defining Regions of Interest for testing reflexive reorientation of attention to external events

We first used the Signal (Stop + Continue) > Go contrast in the group-level GLM analysis to identify lateral prefrontal regions that showed significant activation. Next, we used the same anatomical "mask" for right inferior frontal gyrus (rIFG) that was described above. The region of interest (ROI) was defined as the overlapping area between the functionally defined lateral prefrontal region and the anatomical mask of rIFG. We extracted the beta weights of the ROI, averaged across all voxels in the ROI, for each participant for the following three regressor/contrasts: 1) Go trials alone, 2) Stop - Go trials, and 3) Continue - Go trials. Positive value indicates greater BOLD activity.

Defining FEF

We used frontal eye fields (FEF) as an "area of reference" to assess the validity of the pattern classification method and to benchmark its result with the results found in rVLPFC, since it is well-established that the activation in FEF is associated with oculomotor control (Schiller et al., 1987; Goldberg and Bushnell, 1981; Hanes and Schall, 1996; Connolly et al., 2005; Curtis et al., 2005). FEF was initially identified functionally by selecting voxel clusters from both left and right hemispheres that showed significant activation using the Go – baseline > 0 contrast from the group-level GLM analysis. Second, among the functionally defined regions, only areas that were anterior to the precentral sulcus, and lateral to the superior frontal sulcus were further included in the data analysis (Courtney et al., 1996).

Multi-voxel pattern classification analysis (MVPA)

MVPA (Norman et al., 2006) was performed using a linear support vector machine (LinearCSVMC) from LIBSVM library (Chang and Lin, 2001) implemented within the PyMVPA software package (Hanke et al., 2009). Preprocessing was the same as described above in the GLM analysis. To reduce the problem related to BOLD signals overlapping across temporally adjacent events, a univariate GLM analysis was conducted to derive trial-type-specific beta estimates for each run, representing each possible combination of the two colors (blue and yellow) and three trial types (Go, Stop, and Continue trials). In addition, six head-motion parameters were included in the model as regressors-of-no-interest. Trials were modeled as events time-locked to the onset of the target with a double-gamma function and were convolved with a canonical HRF. Error Go and Continue trials were excluded from analyses.

To test signal meaning encoding, the context rule was defined as the mapping between the meaning of the signal and the color. For each participant, beta values pertaining to each combination of color and meaning were estimated, within each run, yielding four beta maps per run (i.e., "blue Continue," "blue Stop," "yellow Continue," and "yellow Stop"). Overall, the GLM analysis yielded 24 (4 beta maps/run x 6 runs) beta maps for each participant. We then pooled all 21 participants' classification accuracy values and tested them against the chance performance value of 0.5 (because the signal-response mapping meaning was either correctly or incorrectly interpreted by the participant's classifier), at the level of $p < 0.05$ (two-tailed).

A different univariate GLM analysis was conducted to derive stop-outcome-specific beta estimates for each run, representing Failed Stop and Successful Stop outcomes. In addition, six head-motion parameters were included in the model as regressors-of-non-interest. Trials were modeled as events time-locked to the onset of the target with a double-gamma function and were convolved with a canonical HRF. For each participant, beta values pertaining to both trial outcomes were estimated within each run, yielding two beta maps per run. Overall, the GLM analysis yielded 12 (2×6 runs) beta maps.

Task-dependent Functional Connectivity

A generalized form of context-dependent psychophysiological interactions (gPPI) method (McLaren et al., 2012; Cisler et al., 2013) was used with implementations in AFNI. The three seed regions were the ventral rVLPFC, dorsal rVLPFC and bilateral FEF, which were defined at the group-level analysis and transformed back to individual space using 3dNwarpApply in AFNI. For each seed, changes in BOLD signal were modeled to test the effect of modulation in other parts of the brain by the seed region during Go, Stop, and Continue trials.

For each run, the average time series of the voxels in a seed region was extracted, and a deconvolution process was run on the time series to remove the signal component that had previously been modeled with a canonical hemodynamic response function (HRF). The remaining residual signals were considered the neuronal responses at the seed region and were convolved with the condition timing profile for each task, i.e., Go, Stop, and Continue trials, respectively, to generate three PPI-regressors per run. Next, the three PPI-regressors were concatenated across all six runs respectively. In addition to the three PPI-regressors, three regressors of trial types (Go, Stop, and Continue), the seed region itself, and six head-motion parameters were included in the model. All 13 regressors were convolved with the canonical HRF using a double gamma function. The general linear model (GLM) was estimated for each participant separately using AFNI's 3dDeconvolve function, and a Talairach transformation was applied for each participant to combine the resulting statistical maps across the 21 participants for group-level analysis. All contrasts created at the participant-level were entered into a group-level random-effects analysis using a one-sample t test against a contrast value of zero at each voxel. The statistical maps were thresholded using a voxel-level threshold of $p < 0.01$, corrected for multiple comparisons at a cluster-level of $p < 0.05$ (family-wise error correction), based on a Monte Carlo simulation with 10,000 iterations run via the AFNI software package, using a smoothing kernel of 4 mm on the task-related mask.

Primate electrophysiology experiment

Spike density functions

To represent neural activity as a continuous function, we calculated spike density functions by convolving the peri-stimulus time histogram with a growth-decay exponential function that resembled a postsynaptic potential (Hanes et al., 1998). Each spike therefore exerts influence only forward in time. The equation describes rate (R) as a function of time (t): $R(t) = (1 - \exp(-t/\tau_g))*\exp(-t/\tau_d)$, where τ_g is the time constant for the growth phase of the potential and τ_d is the time constant for the decay phase. Based on physiological data from excitatory synapses, we used 1 ms for the value of τ_g and 20 ms for the value of τ_d (Sayer et al., 1990).

Behavioral data analysis

We termed five trial types to characterize the possible behavioral results: Go trials, in which the monkey successfully made a saccade to the periphery target; Successful Stop trials, in which the monkey successfully withheld its gaze at the central fixation; Failed Stop trials, in which the monkey failed to hold central fixation and generated a saccade to the target instead; Continue trials, in which the monkey successfully ignored the continue signal, and generated a saccade to the target; and Error Continue trials, in which the monkey failed to generate a saccade to the target and held its gaze at central fixation instead. Inhibition function and stop signal reaction time (SSRT) were calculated using a similar method as in the human fMRI study.

Characterization of neuronal activity dynamics

See Table S8.

For a neuron to sufficiently control a saccade initiation or inhibition, two criteria must be fulfilled. First, the neuron must discharge differently when a saccade is initiated versus when a saccade is withheld. Second, this activity differentiation must occur within the SSRT for it to control the saccade initiation/inhibition in time. If the activity differentiates after the SSRT, it is too late to influence the saccade initiation/inhibition. Both criteria are fulfilled by movement-related neurons in the FEF and superior colliculus (SC) (Brown et al., 2008; Hanes et al., 1998; Paré and Hanes, 2003).

The activity when a movement is cancelled can be compared with the activity when a movement is produced, but would have been cancelled if the stop signal had been presented. This comparison consists of Successful Stop trials and Go trials with reaction times greater than the stop signal reaction time added to the stop signal delay (latency-matched trials). The rationale is that the saccades, generated with slow reaction times (i.e., reaction times exceeding the SSRT + SSD) in Go trials, are those slow saccades that could have afforded enough time for the STOP process to finish before the GO process, and on which the planned movement therefore would have been cancelled had there been a stop signal presented.

We compared the spike rate in Successful Stop trials and latency-matched Go trials for movements inside and outside of the response fields as a function of time from target presentation. This was done to provide a complementary estimate of whether and when neural activity distinguished saccade inhibition from saccade initiation. To perform this time-course analysis, we subtracted the average spike density function for Successful Stop trials from the average spike density function for latency-matched Go trials. This subtraction was performed for cells with visually evoked activity and for cells with movement-related activity. Because of their opposite sign of modulation, for cells with fixation-related activity, we subtracted the average spike density function for latency-matched Go trials from the average spike density function during cancelled Stop trials. The resulting spike density functions will be referred to as differential spike density functions. The time at which significant differential activity began during Successful Stop and latency-matched Go trials was defined as the instant when the differential spike density function exceeded by 2 SD the mean difference in activity during the 500-ms interval before target presentation, provided the difference reached 3SD and remained > 2 SD threshold for 50ms. The time interval between the defined onset of differential activity and the SSRT then was

determined. If the time when the differential activity arose was earlier than or equal to the SSRT, we regarded this as positive evidence for a cancellation signal.

Identification of context related neuronal activity

We used a method adopted from signal detection theory (Green and Swets, 1966) to determine when the activity evoked by a stimulus in one context could be distinguished from the activity evoked by the same stimulus in another context. To do this, we compared the distribution of discharge rates during the 100 ms interval following each behavioral event (e.g., context cue, target, stop signal, reward).

At each time interval, the separation of the two distributions of activity obtained when a trial occurred during context A versus when a trial occurred during context B was quantified by calculating receiver operating characteristic (ROC) curves (Egan, 1975; Green and Swets, 1966; Macmillan and Creelman, 2004). This method has previously been used to analyze the ability of single neurons to discriminate stimulus features (e.g., Bradley et al., 1987; Britten et al., 1992; Guido et al., 1995; Tolhurst et al., 1983; Vogels and Orban 1990; Zohary et al., 1990). Significant differences in activity between contexts were determined by plotting ROC curves for the activity distribution in the 100 ms interval following each behavioral event. Each neuron with a time epoch where the area under the ROC curve exceeded 0.75 was defined as having significant context related modulation.

Classification of Stop and Continue Responses

We analyzed the pattern of neuronal activity following stop and continue signals using a 2-factor ANOVA. One factor was trial type (cancelled stop signal trial, non-cancelled stop signal trial, continue trial), the other context (A or B), and their interaction. We distinguished between correct and erroneous stop signal trials and continue trials. Since the monkey almost always correctly responded to continue signals by generating a saccade, we did not analyze erroneous continue trials. We conducted this ANOVA on activity in each of 14 non-overlapping 50 ms time bins that covered the time period from 200 ms before signal onset until 400 ms past signal onset. If one of the factors had a significant effect in two consecutive time bins ($p < 0.0025$), we conducted post hoc comparisons of the neuronal activity in these bins sorted by the relevant factor.

Break down of neuronal profile in rVLPFC (right area 44/45)

A total number of 326 rVLPFC neurons were recorded and 313 (96%) showed task related activity. Of the 313 neurons, 37 (11.8%) neurons were with saccade related activity, 15 with visual related activity (4.8%), 48 (15.3%) with visual-movement related activity and 196 (62.6%) with context-related activity. From the 85 movement related neurons (combing both visual and visual-movement neurons), there were 557 stop signal delays with sufficient trials to measure cancellation time. Of these there were 365 stop signal delays where there was no significant difference in firing rate when comparing latency matched Go trials to SS trials. Of the 192 stop signal delays where there was a significant difference in firing rate when comparing latency matched Go trials to SS trials, 167 of those significant differences in firing rate occurred well after the SSRT had elapsed (80.32 ± 10.94 ms). The distribution of these cancellation times relative to the SS was significantly greater than 0 ($t(191) = 10.17$, $p = 1.09e\text{-}19$).

DATA AND SOFTWARE AVAILABILITY

All data are freely available upon request. For human fMRI data contact Susan Courtney (courtney@jhu.edu). For monkey electrophysiological data contact Veit Stuphorn (veit@jhu.edu).